Stem Cell Reports
Article

ISSCR

OPEN ACCESS

GRM7 Regulates Embryonic Neurogenesis via CREB and YAP

Wenlong Xia,[1,2] YanLi Liu,[1] and Jianwei Jiao[1,*]
[1]State Key Laboratory of Reproductive Biology, Institute of Zoology, Chinese Academy of Sciences, Beijing 100101, China
[2]School of Life Sciences, University of Science and Technology of China, Hefei, Anhui 230026, China
*Correspondence: jwjiao@ioz.ac.cn
http://dx.doi.org/10.1016/j.stemcr.2015.03.004

SUMMARY

Metabotropic glutamate receptor 7 (GRM7) has recently been identified to be associated with brain developmental defects, such as attention deficit hyperactivity disorder (ADHD) and autism. However, the function of GRM7 during brain development remains largely unknown. Here, we used gain- and loss-of-function strategies to investigate the role of GRM7 in early cortical development. We demonstrate that *Grm7* knockdown increases neural progenitor cell (NPC) proliferation, decreases terminal mitosis and neuronal differentiation, and leads to abnormal neuronal morphology. GRM7 regulates the phosphorylation of cyclic AMP response element-binding protein (CREB) and the expression of Yes-associated protein (YAP) by directly interacting with CaM, which subsequently regulates the expression of *CyclinD1* and ultimately affects early cortical development. These defects in neurogenesis are ameliorated by *Grm7* overexpression, *Creb* knockdown, or *Yap* knockdown. Thus, our findings indicate that GRM7 signaling via CREB and YAP is necessary for neurogenesis in the brain.

INTRODUCTION

The complex structure of the mammalian cerebral cortex is derived from neuroepithelial (NE) cells in the neural tube (McConnell, 1995). NE cells give birth to multiple progenitor populations (Götz and Huttner, 2005; McConnell, 1995). There are two germinal zones in the embryonic neocortex: the ventricular zone (VZ) and the subventricular zone (SVZ) (Gal et al., 2006). Radial glial (RG) cells give rise to self-renewing cells and produce intermediate progenitor (IP) cells via asymmetrical division. IP cells subsequently divide into two neurons via symmetrical division (Götz and Huttner, 2005; McConnell, 1995; Rakic, 1995). During the process of progenitor cell transformation into mature neurons, the precise control of the timing of self-renewal, differentiation, neuronal migration, and neuronal maturation of neural progenitor cells (NPCs) is required (Xu et al., 2014). Therefore, it is not surprising that mistakes in this process of early cortical development lead to serious consequences, such as autism spectrum disorder (ASD) and attention deficit hyperactivity disorder (ADHD).

Metabotropic glutamate receptor 7 (GRM7) is defined as an ASD- (Yang and Pan, 2013) and ADHD-related gene (Elia et al., 2012) and is exclusively expressed in the CNS (Bradley et al., 1996). Metabotropic glutamate receptors are potential targets for neuropsychiatric disorders (Dev, 2004) that modulate neurotransmitter release and neuronal excitability (Schlett, 2006). Metabotropic glutamate receptors are subdivided into groups I (GRM1 and GRM5), II (GRM2 and GRM3), and III (GRM4, GRM6, GRM7, and GRM8) on the basis of homology, intracellular messengers, and ligand selectivity (Schlett, 2006). Characteristic of all metabotropic glutamate receptors, the GRM7 protein is localized to the neuronal presynaptic membrane, and its protein sequence is highly conserved (Bradley et al., 1996). These findings suggest that GRM7 may play an important and irreplaceable role in the nervous system. However, its role in the process of cortical development is unclear.

During neurogenesis, cyclic AMP response element-binding protein (CREB) is involved in multiple aspects of neuronal development and plasticity, including cell survival, proliferation, and differentiation (Mantamadiotis et al., 2012). CREB is expressed throughout neurogenesis (Giachino et al., 2005), and a previous study has shown that neural proliferation defects result from the alteration of CREB activity during early development (Dworkin et al., 2007). Yes-associated protein (YAP) modulates organ size by regulating cell apoptosis and proliferation (Cai et al., 2010; Lian et al., 2010). YAP is expressed in mitotic neuronal progenitors, and it is downregulated during neuronal differentiation (Zhang et al., 2012). The phosphorylation of YAP at Ser127 results in a loss of function and the subsequent repression of downstream target genes, leading to premature neuronal differentiation (Cao et al., 2008). In the absence of inhibitory phosphorylation, YAP promotes cell proliferation and suppresses cell differentiation (Zhang et al., 2012). During neurogenesis, CYCLIND1 plays an important role in neural progenitor proliferation; when CYCLIND1 is constitutively activated, the proliferation of NPCs is increased (Das et al., 2010). To investigate the function of GRM7 in early cortical development, we downregulated its expression in neuronal progenitor cells of the cerebral ventricle of embryos via in utero electroporation (IUE). We determined that *Grm7* knockdown increases the proliferation of PAX6-positive RG cells, decreases the amplification of TBR2-positive IP cells, and

results in a reduction in the number of progenitor cells that differentiate into neurons. Furthermore, morphological maturation was seriously affected by the silencing of *Grm7*. We also demonstrated that *Creb* or *Yap* knockdown ameliorates the *Grm7* knockdown phenotype in vivo. Overall, our findings suggest that GRM7 regulates the phosphorylation of CREB and the expression of YAP in neuronal progenitor cells, affecting the expression of *CyclinD1*, which ultimately controls neuronal differentiation and maturation during cortical development.

RESULTS

GRM7 Is Expressed in Neural Progenitor Cells

During cortical development, GRM7 displays a specific temporal and spatial expression pattern. To determine whether the GRM7 protein is expressed in brain tissue during different developmental periods, we performed western blot to analyze its expression pattern. Our results showed that the GRM7 protein expressed was already detectable at embryonic day 12.5 (E12.5), gradually increased until E15.5, and then dramatically decreased between E15.5 and E18.5 (Figure 1A). This finding suggests that GRM7 may play an important role in early embryonic cortical development. Neocortical sections of E12.5, E15.5, and E18.5 mouse brains were collected and immunostained for GRM7, and the results showed that its expression pattern was dynamic in the VZ/SVZ. At E12.5, in which the cerebral cortex is primarily composed of NPCs, we determined that the GRM7 protein was expressed throughout the cortex. At E15.5, GRM7 protein was highly expressed in the VZ/SVZ. However, at E18.5, which is near the end of the embryonic neurogenesis period, the expression of GRM7 in the cerebral cortical plate was higher than that in the VZ/SVZ (Figure 1B). In the embryonic cerebral cortex, we determined that the GRM7 protein colocalized with NESTIN- and PAX6-positive neuronal progenitor cells residing in the VZ/SVZ at E15.5 (Figures 1C and 1D). Moreover, we determined that GRM7 colocalized with NESTIN- and PAX6-positive cultured neuronal progenitor cells, which were isolated from E12.5 mouse brains and cultured in proliferative medium for 24 hr (Figures S1A and S1B). Additionally, based on in situ hybridization, *Grm7* was expressed in the VZ/SVZ of the neocortex (Figure S1C). For further experiments, we generated two *Grm7*-specific short hairpin RNA (shRNA) (*Grm7*shRNA-1 and *Grm7*shRNA-2) plasmids and a *Grm7* overexpression plasmid to efficiently silence or overexpress GRM7 expression, respectively, in embryonic NPCs (Figures 1E and 1F).

Grm7 knockdown decreased the immunostaining for GRM7 in E16.5 brain sections following the electroporation of the *Grm7*shRNA-1 or *Grm7*shRNA-2 plasmid into the embryonic brains at E13.5 (Figures 1G and 1H). A similar result was obtained in cultured NPCs transfected with these knockdown plasmids in vitro (Figure S1D).

Overall, the specific temporal and spatial expression pattern of GRM7 suggests that GRM7 may be involved in the regulation of the proliferation and differentiation of NPCs during early cortical development.

GRM7 Regulates Neural Progenitor Proliferation in the Brain

To study the functional role of GRM7 in neurogenesis, we investigated NPCs proliferation in vivo based on its expression in neural progenitor cells via IUE. The control or *Grm7* shRNA plasmid was electroporated into E13.5 mouse brains, which were collected 72 hr later for phenotypic analysis. Analysis of the distribution of GFP-positive cells revealed that *Grm7* knockdown caused an augmentation of GFP-positive cells in the VZ/SVZ and a corresponding reduction in GFP-positive cells in the cortical plate (CP). In the intermediate zone (IZ), the GFP-positive cell number did not change (Figures 2A and 2B).

To further explore the effects of GRM7 on NPC proliferation, we injected pregnant dams with bromodeoxyuridine (BrdU) 2 hr prior to collecting the electroporated brains. The knockdown of *Grm7* led to an increase in GFP and BrdU double-positive neural progenitor cells (Figures 2C and 2D) and in the mitotic index in the VZ/SVZ (Figures S2A and S2B). We employed an in vitro culture system to assess the function of GRM7 in neuronal proliferation. Neural progenitor cells were isolated from E12.5 mouse brains and cultured for 1 day; then, the cells were infected with either control or *Grm7* shRNA lentivirus. The infected cells were cultured for 3 days under proliferative conditions. Then, 5-ethynyl-2′-deoxyuridine (EdU) was added to the culture medium for 2 hr. The quantification of GFP and EdU double-positive cells revealed that the knockdown of *Grm7* in vitro increased neuronal proliferation compared with the control treatment (Figure S2C).

To investigate the specific cell groups of proliferative progenitor cells in the VZ/SVZ, we selected two types of neural progenitor cell markers: PAX6 and TBR2. During the process of early brain development, PAX6-positive RG cells divide asymmetrically to self-renew and generate TBR2-positive IP cells or neurons. Subsequently, IP cells divide symmetrically to produce two neurons (Götz and Huttner, 2005). Our results showed that *Grm7* knockdown significantly increased the proportion of PAX6-positive RG cells (Figures 2E and 2F) at the expense of TBR2-positive IP cells (Figures 2G and 2H). We also determined that *Grm7* knockdown had no effect on the apoptosis of neural progenitor cells (Figure S3A). Further analysis showed that the proportion of GFP-BrdU-PAX6-positive cells was increased (Figures S3B and S3C) but that the proportion

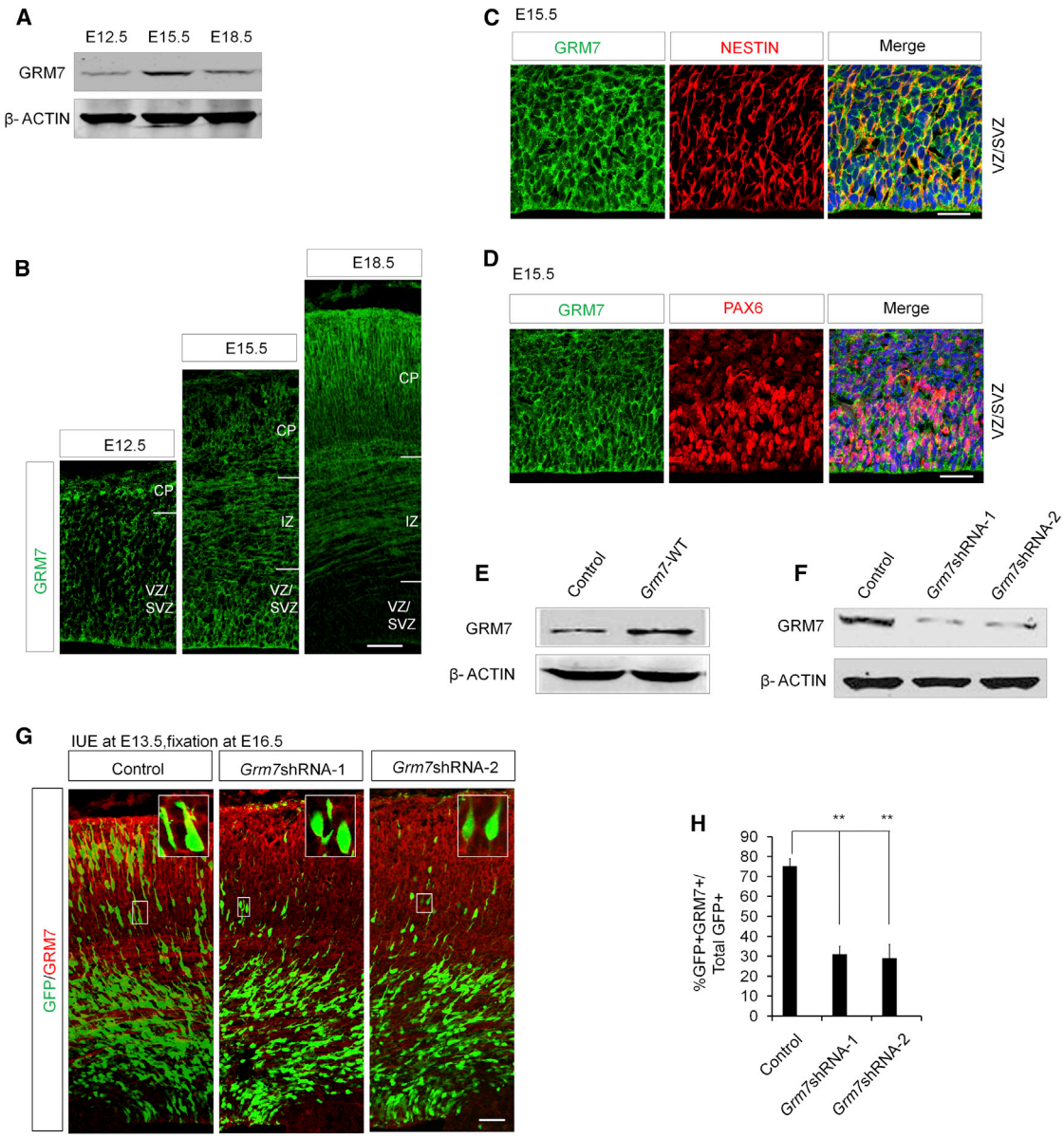

Figure 1. GRM7 Is Expressed in Embryonic Neural Progenitor Cells

(A) Western blot analysis of cortical lysates collected at various time points (E12.5, E15.5, or E18.5).

(B) GRM7 expression in the mouse cortex. Cortical sections of were collected from mice at E12.5 (left), E15.5 (middle), or E18.5 (right) and were stained for GRM7. The scale bar represents 50 μm.

(C) E15.5 embryonic brain sections were co-stained with anti-GRM7 and anti-NESTIN antibodies (VZ/SVZ). The scale bar represents 25 μm.

(D) E15.5 embryonic brain sections were co-stained with anti-GRM7 and anti-PAX6 antibodies. The scale bar represents 25 μm.

(E and F) Western blot analysis shows the overexpression (empty PCDH expression vector as a control) or the knockdown of *Grm7* (empty pSicoR shRNA vector as control).

(G and H) *Grm7* knockdown decreased the proportion of GRM7-GFP double-positive cells in utero. The control or *Grm7* shRNA plasmid was electroporated into E13.5 embryonic mouse brains, and the mice were sacrificed at E16.5. The percentage of GRM7-GFP double-positive cells is shown (n = 3 independent experiments; error bars represent mean ± SEM; **p < 0.01). The scale bar represents 50 μm.

See also Figure S1.

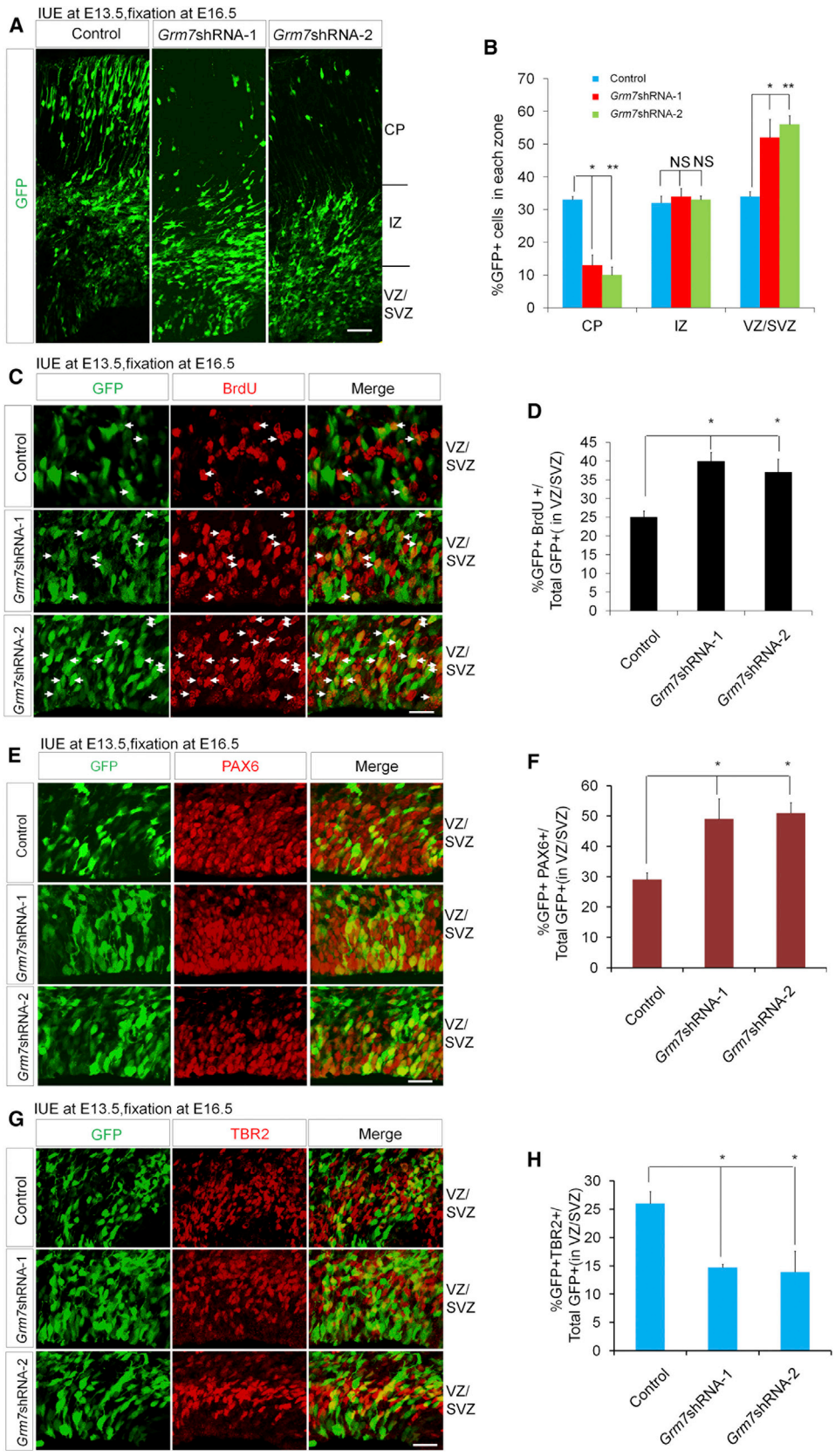

(legend on next page)

of GFP-BrdU-TBR2-positive cells was decreased (Figures S3D and S3E) in the embryonic brain after electroporation with a *Grm7*-knockdown plasmid compared to the control plasmid. These data indicate that GRM7 loss of function may cause an augmentation of proliferative cells located in the VZ/SVZ.

Grm7 Knockdown Inhibits Cell-Cycle Exit by Neural Progenitor Cells and Neuronal Differentiation

Our observations that *Grm7* knockdown increased neural progenitor proliferation and the number of GFP-positive cells in the VZ/SVZ suggest that the differentiation of NPCs into neurons may be affected by *Grm7* knockdown. To test this possibility, we performed cell-cycle exit analysis following IUE at E13.5. BrdU was injected into pregnant dams at E15.5, 2 days after IUE, and the electroporated brains were collected at E16.5 and subjected to immunohistochemistry for BrdU and Ki67. Based on this analysis, we determined that *Grm7* knockdown caused a significant decrease in the proportion of $GFP^+BrdU^+Ki67^-$ cells relative to that of GFP^+BrdU^+ cells in the VZ/SVZ (Figures 3A and 3B), which implied that *Grm7* knockdown resulted in a decreased number of neural progenitor cells that exit the cell cycle.

To investigate whether this intervention directly leads to reduced neuronal differentiation, we stained electroporated brain sections with an anti-neuronal bIII-tubulin (TUJ1) antibody. The quantification of GFP and TUJ1 double-positive cells revealed that *Grm7* knockdown led to a significant decrease in the percentage of GFP and TUJ1 double-positive cells, demonstrating that the loss of GRM7 expression resulted in a decrease in neuronal differentiation (Figures 3C and 3D).

We also employed an in vitro culture system to assess the function of GRM7 in neurogenesis. Neural progenitor cells were isolated from E12.5 mouse brains and cultured for 1 day; the cells were then infected with either control or *Grm7* shRNA lentivirus. The infected cells were cultured for 3 days under differentiating conditions, and neuronal differentiation was subsequently assessed by co-staining with anti-GFP and anti-TUJ1 antibodies. The quantification of GFP and TUJ1 double-positive cells revealed that the knockdown of *Grm7* in vitro decreased neuronal differentiation compared with the control treatment (Figures 3E and 3F).

Grm7 Knockdown Prohibits the Terminal Mitosis of NPCs

To determine whether GRM7 regulates premature NPCs terminal mitosis to control the differentiation process during early cortical development, we conducted a BrdU birthdating study (Duque and Rakic, 2011). As shown in the timeline, a single BrdU injection was administered to pregnant dams 1 day after electroporation, and the electroporated brains were collected 5 days after electroporation (Figure 4A). Because BrdU only labels cells that are in the process of proliferation and in the S phase of mitosis (Nowakowski et al., 1989), cells in their final mitotic division at the time of BrdU administration become permanently labeled with BrdU and progress toward neuronal differentiation and migration to the cortical plate. However, BrdU becomes diluted with each mitotic cycle in continually proliferating NPCs; thus, BrdU cannot be detected using an anti-BrdU antibody in continually proliferating NPCs on E18.5 (Hasan et al., 2013). The quantification of the percentage of double-labeled ($BrdU^+GFP^+$) cells in all cortical layers revealed a significant decrease in newly born neurons in *Grm7* shRNA plasmid-electroporated brains compared with the control shRNA plasmid-electroporated brains from littermates (Figures 4B–4E). These results indicate that *Grm7* knockdown inhibits premature NPCs terminal mitosis, thereby decreasing neural differentiation.

Figure 2. GRM7 Regulates Neural Progenitor Cell Proliferation

(A and B) *Grm7* knockdown causes GFP-positive cell positioning defects in utero. The empty shRNA control or *Grm7* shRNA plasmid was electroporated into E13.5 embryonic mouse brains, and the mice were sacrificed at E16.5. The percentage of GFP-positive cells in each region is shown (n = 3 independent experiments; error bars represent mean ± SEM; *p < 0.05, **p < 0.01). The scale bar represents 50 μm. CP, cortical plate; IZ, intermediate zone; VZ/SVZ, ventricular zone/subventricular zone.

(C and D) BrdU incorporation is increased in *Grm7* shRNA plasmid-electroporated brains. The brains of mice electroporated at E13.5 were injected with BrdU (100 mg/kg, i.p.) for 2 hr prior to sacrificing at E16.5. The white arrows indicate GFP and BrdU double-positive cells. The bar graph shows the percentage of BrdU and GFP double-positive cells relative to the total GFP-positive cells in the VZ/SVZ (n = 3 independent experiments; *p < 0.05, **p < 0.01; error bars represent mean ± SEM). The scale bar represents 20 μm.

(E and F) PAX6 and GFP double-positive cells are increased in *Grm7* shRNA plasmid-electroporated brains. Cerebral cortical sections collected 3 days after electroporation with either the control or *Grm7* shRNA plasmid at E13.5 were stained for PAX6. The bar graph shows the percentage of PAX6 and GFP double-positive cells relative to the total GFP-positive cells in the VZ/SVZ (n = 3 independent experiments; *p < 0.05, **p < 0.01; error bars represent mean ± SEM). The scale bar represents 20 μm.

(G and H) TBR2 and GFP double-positive cells are decreased in the *Grm7* shRNA plasmid-electroporated brains. Brain sections at 3 days after electroporation with either the control or *Grm7* shRNA plasmid at E13.5 were stained for TBR2. The bar graph shows the percentage of TBR2 and GFP double-positive cells relative to the total GFP-positive cells in the VZ/SVZ (n = 3 independent experiments; *p < 0.05, **p < 0.01; error bars represent mean ± SEM). The scale bar represents 20 μm.

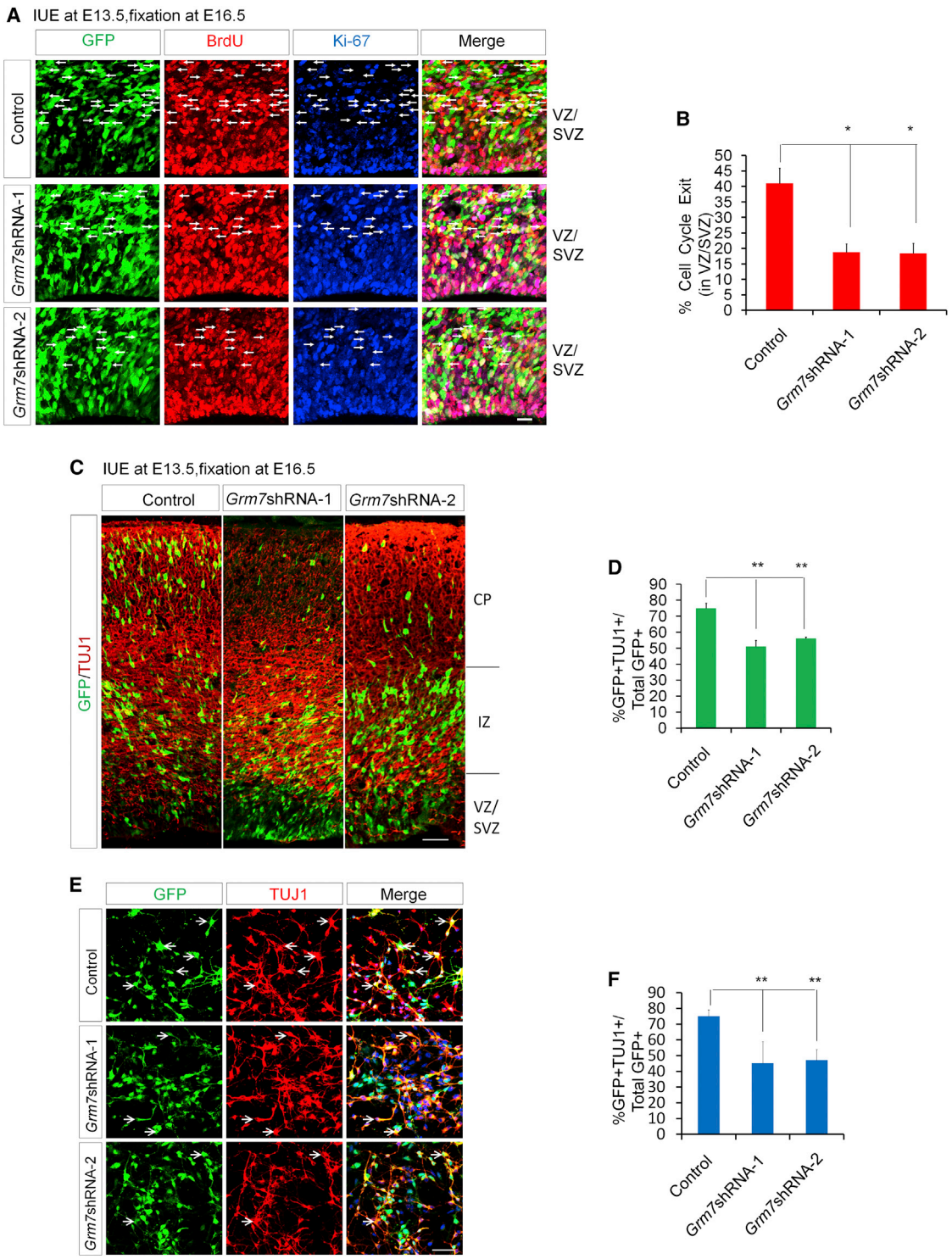

Figure 3. *Grm7* Knockdown Inhibits Neural Progenitor Differentiation

(A and B) *Grm7* knockdown in progenitor cells reduces premature cell cycle exit in utero. The empty shRNA control or *Grm7*-shRNA plasmid was electroporated into E13.5 embryonic brains, and BrdU was injected at E15.5. The mice were sacrificed at E16.5. The cell-cycle exit index was calculated as the percentage of GFP-positive cells that exited the cell cycle ($GFP^+BrdU^+Ki67^-$) divided by the total GFP and BrdU double-positive (GFP^+BrdU^+) cells. The white arrows indicate $GFP^+BrdU^+Ki67^-$ cells. The bar graph shows the percentage of

(legend continued on next page)

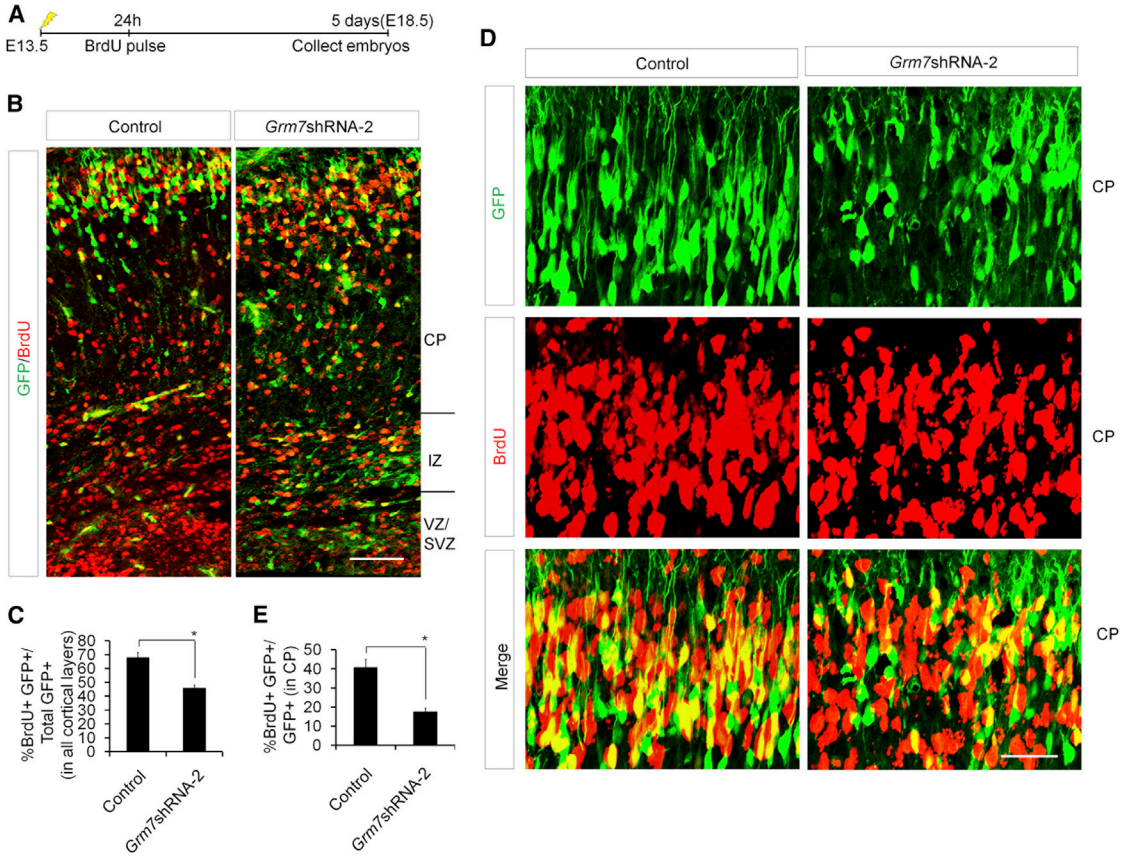

Figure 4. GRM7 Is Required for Neural Progenitor Terminal Mitosis

(A) Timeline of the BrdU birth-dating experiment. The control or *Grm7* shRNA plasmid was electroporated into E13.5 embryonic mouse brains. BrdU was injected 24 hr after electroporation, and the brains were collected 5 days after electroporation.

(B and D) Low- (B) and high-magnification (D) confocal images of brain sections from control or *Grm7* shRNA plasmid-electroporated mice immunostained with an anti-BrdU antibody. The white arrows indicate GFP and BrdU double-positive cells. The scale bar represents 50 μm (B) or 25 μm (D).

(C and E) The bar graph shows the percentage of BrdU and GFP double-positive cells relative to total GFP-positive cells in all cortical layers or in the CP (n = 3 independent experiments; *p < 0.05, **p < 0.01; error bars represent mean ± SEM).

Grm7 Knockdown Leads to Persistent Abnormal Neuronal Development

To further determine the role of GRM7, we performed long-term tracing of GFP cells during cortical development. The control or *Grm7* shRNA plasmid was electroporated into E13.5 mouse brains, and the brains were collected 5 days later at E18.5. Compared with the control group, the GFP-positive cell distribution was altered in the *Grm7*-knockdown group. The number of GFP-positive cells was reduced in the CP and the IZ but increased in the VZ/SVZ

$GFP^+BrdU^+Ki67^-$ cells relative to the total BrdU and GFP double-positive cells in the VZ/SVZ (n = 3 independent experiments; *p < 0.05, **p < 0.01; error bars represent mean ± SEM). The scale bar represents 20 μm.

(C and D) *Grm7* knockdown decreases neuronal differentiation in vivo. E16.5 brain sections were stained for TUJ1 after the electroporation of the control or *Grm7*-shRNA plasmid into the brain on E13.5. The quantification of the percentage of GFP and TUJ1 double-positive cells relative to the total GFP-positive cells is shown as a bar graph (n = 3 independent experiments; *p < 0.05, **p < 0.01; error bars represent mean ± SEM). The scale bar represents 50 μm.

(E and F) *Grm7* knockdown decreases neuronal differentiation in vitro. Neural progenitor cells were isolated from E12.5 mouse brains and cultured for one day; the neural progenitor cells were subsequently infected with either the control or *Grm7* shRNA lentivirus. The quantification of the percentage of GFP and TUJ1 double-positive cells relative to total GFP-positive cells is shown as a bar graph (n = 3 independent experiments; *p < 0.05, **p < 0.01; error bars represent mean ± SEM). The scale bar represents 25 μm.

See also Figures S2 and S3.

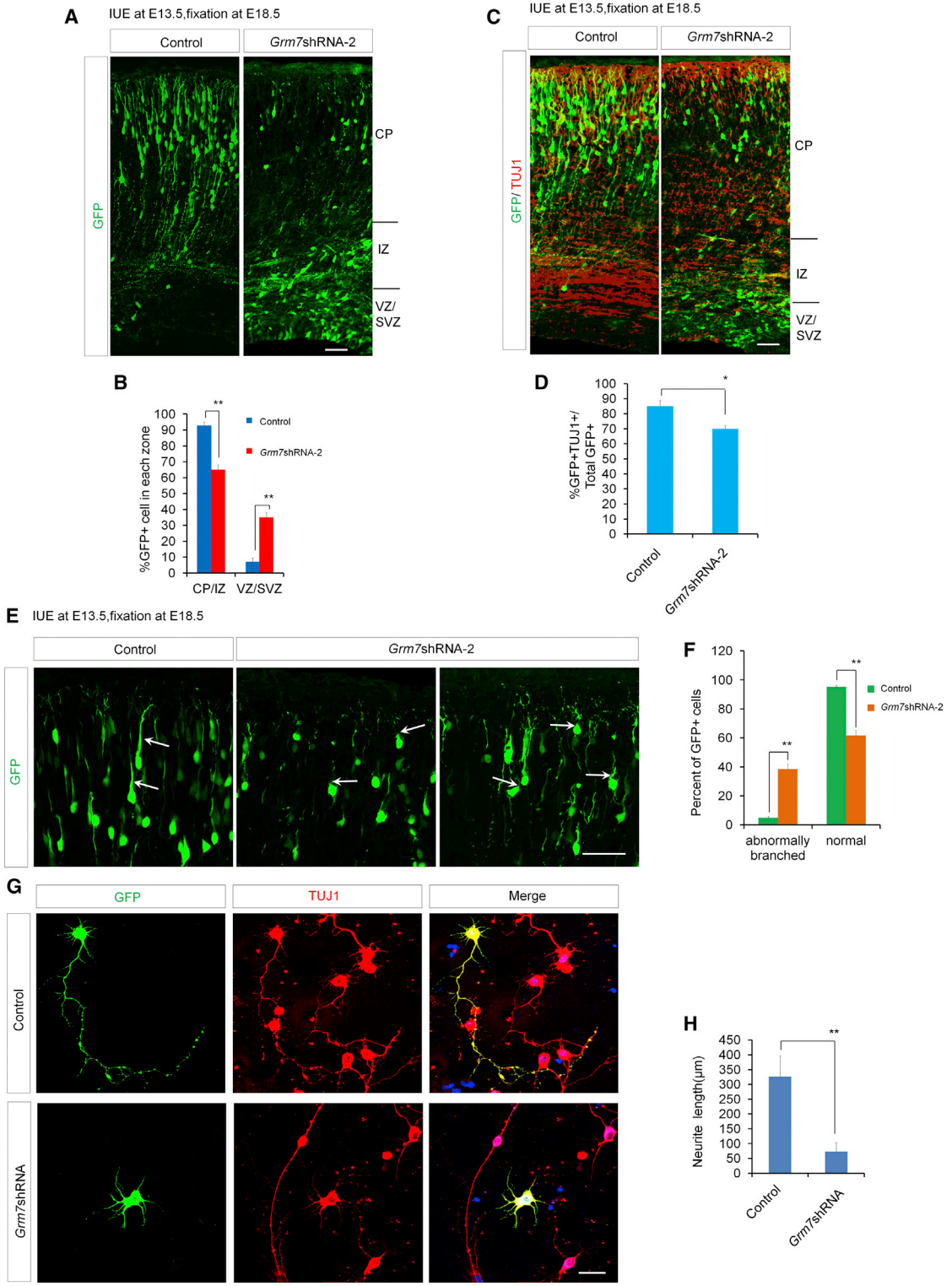

Figure 5. *Grm7* Knockdown Affects Neuronal Development

(A and B) *Grm7* knockdown causes GFP-positive cell positioning defects in vivo. The control or *Grm7*-shRNA plasmid was electroporated into E13.5 embryonic mouse brains, and the mice were sacrificed at E18.5. The percentage of GFP-positive cells in each region is shown (n = 3 independent experiments; *p < 0.05, **p < 0.01; error bars represent mean ± SEM). The scale bar represents 20 μm.

(legend continued on next page)

(Figures 5A and 5B). The precocious or suppressed neuronal differentiation upon *Grm7* knockdown ultimately resulted in a reduced number of TUJ1-positive upper-layer cortical neurons at E18.5 (Figures 5C and 5D). Based on further observation of high-resolution images, we determined that *Grm7* knockdown substantially induced abnormal neuronal branching in vivo, as reported by a previous study (Zhang et al., 2013). The leading processes in the control group were long and straight, but those in the *Grm7* knockdown group were short and twisted, aberrantly branched, or poorly developed (Figures 5E and 5F), as described in a previous study (Zhang et al., 2013).

In vitro, GFP-positive cells were isolated from brains 24 hr post-electroporation, cultured for 72 hr, and then stained with an anti-neuronal bIII-tubulin (TUJ1) antibody. We observed a significant difference in neuronal morphology between the control and *Grm7*-silenced cells in culture. *Grm7* knockdown resulted in reduced neurite length compared with the control treatment (Figures 5G and 5H). Interestingly, we also determined that the GFP-positive *Grm7*-silenced cells more frequently failed to develop into polarized neurons versus the control cells. In addition, some GFP-positive *Grm7*-silenced cells were round and exhibited very recently completed mitosis (Figure S4A). These results suggest that GRM7 is required for neuronal development.

GRM7 Regulates Neurogenesis via the Modulation CREB and YAP

It has been reported that both CREB (Stachowiak et al., 2003) and YAP (Gee et al., 2011) are expressed in NPCs. Previous studies have shown that GRM7 controls the production of cyclic AMP (cAMP) in the cytoplasm and that CREB plays a critical role in neuronal proliferation via a cAMP-dependent mechanism. We investigated whether there is a relationship between GRM7 and CREB. In vitro, we determined that *Grm7* knockdown increased the phosphorylation of CREB at Ser133. Conversely, *Grm7* overexpression decreased the phosphorylation of CREB at Ser133. YAP acts as an important regulator of brain size and development. Next, we examined whether GRM7 affects YAP signaling. Our results showed that *Grm7* knockdown increased the expression of YAP. Conversely, *Grm7* overexpression decreased the expression of YAP, and subsequent *Grm7* knockdown rescued the phosphorylation of CREB at Ser133 and the expression of the YAP (Figures 6A and 6B).

Because GRM7 is a membrane protein that regulates the flow of calcium ions, we used calmodulin (CaM) to bridge the connection between GRM7 and CREB. We determined that *CaM* overexpression led to an increase in the phosphorylation of CREB at Ser133 and in the expression of YAP; these effects were similar to those of *Grm7* knockdown (Figures 6C and 6D). We further investigated the effects of CREB on YAP. When *Creb* was overexpressed, the expression of YAP was increased (Figure 6E). When *Creb* was silenced, the expression of YAP was decreased (Figure 6F). This result indicates cross-talk between CREB and YAP signaling. To study whether CREB and YAP act in parallel, we electroporated different plasmid combinations into E13.5 mouse brains, and the brains were collected 72 hr later for phenotypic analysis. The results showed that *Creb* overexpression caused a phenotype similar to that of *Grm7* knockdown, and this phenotype was ameliorated by simultaneous *Yap* knockdown. In addition, overexpression of *YAP-S127A*, a constitutively expressed form of YAP, caused abnormalities similar to those caused by *Grm7* knockdown; however, simultaneous *Creb* knockdown failed to ameliorate these abnormalities (Figures 6G and 6H). Therefore, the results indicated that CREB and YAP act downstream of GRM7 and that YAP acts downstream of CREB.

A previous study has reported that the YAP protein accumulates in the nucleus to promote cell proliferation (Fernandez-L et al., 2009). Our results showed that the YAP protein was accumulated in the nucleus upon *Grm7* knockdown (Figures 6I, 6J, S5C, and S5D).

Chromatin immunoprecipitation (ChIP) analysis was then employed, and the results demonstrated that when *Creb* was overexpressed, the amount of CREB that bound to the −0.5-kb region (R1) of the *Yap* promoter was increased (Figures 6K and S5A); the positive region R1 was selected based on a previous study (Wang et al., 2013). The region of R2 was randomly selected as a negative

(C and D) Decreased neuronal differentiation of *Grm7*-silenced cells in vivo. Confocal images of E18.5 brain sections immunostained for TUJ1 after the electroporation of the control or *Grm7*-shRNA plasmid into the brain on E13.5. The quantification of the percentage of GFP and TUJ1 double-positive cells relative to the total GFP-positive cells in all cortical layers is shown as a bar graph (n = 3 independent experiments; *p < 0.05, **p < 0.01; error bars represent mean ± SEM). The scale bar represents 20 μm.

(E and F) High-magnification confocal images of the brain sections show that *Grm7*-knockdown results in the formation of abnormally branched processes compared to the control treatment (n = 3 independent experiments; *p < 0.05, **p < 0.01; error bars represent mean ± SEM). The scale bar represents 20 μm.

(G and H) GRM7 regulates the morphological maturation of neurons in vitro. Images of GFP-positive cells cultured from 1 day post-electroporation brains for 72 hr were immunostained for TUJ1. The quantification of the neurite length is shown as a bar graph (n = 50 cells; *p < 0.05, **p < 0.01; error bars represent mean ± SEM). The scale bar represents 25 μm.

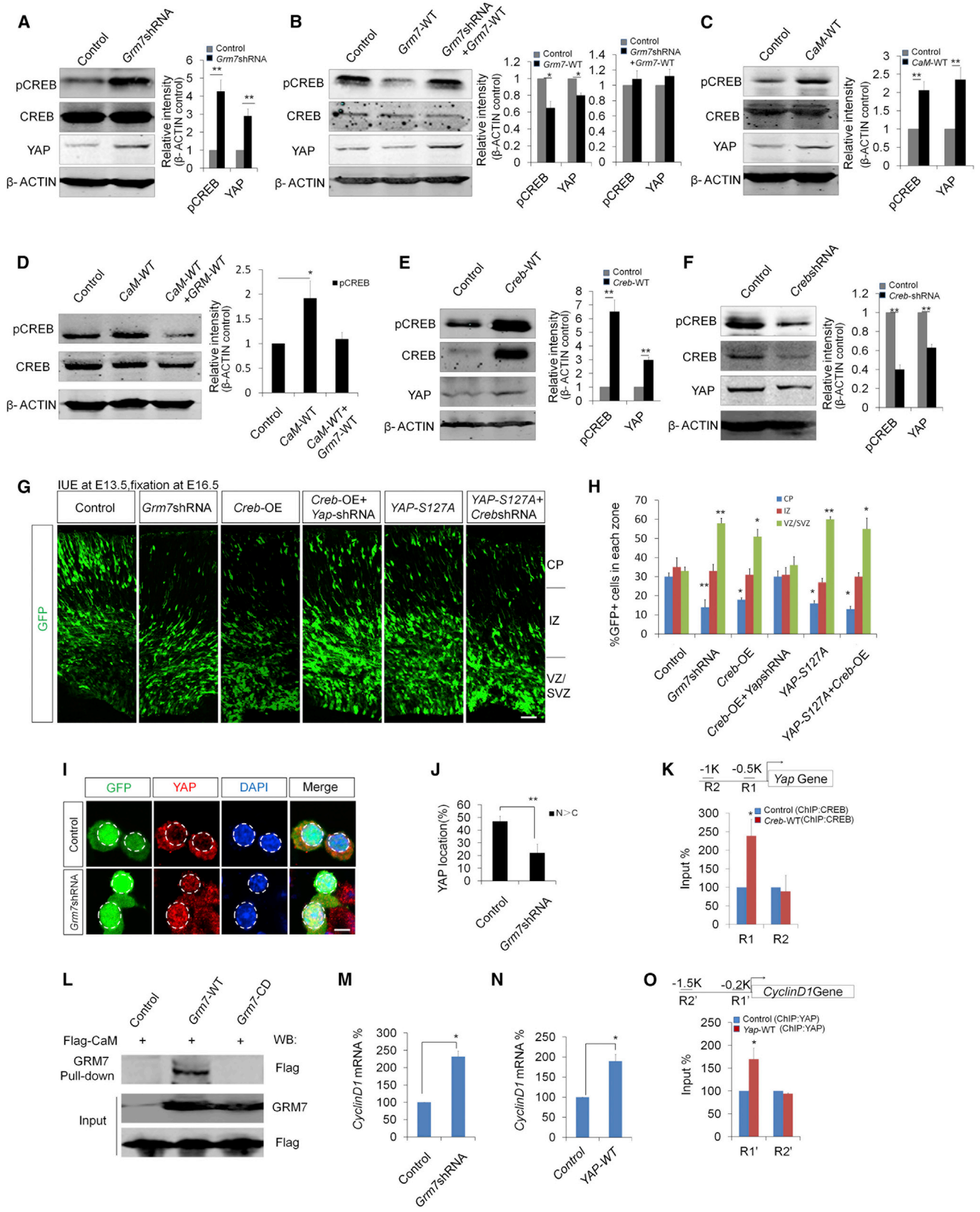

(legend on next page)

unrelated region. The structure of GRM7 has previously been reported (Figure S4B) (Suh et al., 2008). Co-immunoprecipitation was performed to confirm the interaction between GRM7 and CaM. *Grm7* or a control expression plasmid was cotransfected with *Flag-CaM*, and the results indicated that CaM was immunoprecipitated by GRM7. It has been reported that the C-terminal of G protein-coupled receptors is important for signal transduction; therefore, we deleted the C-terminal region of GRM7 to construct the *Grm7-CD* plasmid (Figure S4C). When the C-terminal region of GRM7 was deleted (GRM7-CD), CaM was not immunoprecipitated by GRM7-CD under the identical conditions (Figure 6L).

In our study, we observed that when *Grm7* was silenced, the percentage of cells exiting the cell cycle ($GFP^+BrdU^+Ki67^-$) was decreased. Therefore, real-time PCR was performed to analyze the expression of *CyclinD1*, a cell cycle-related gene. The results showed that when *Grm7* was silenced, the expression of *CyclinD1* was increased, and a similar result was observed when *Yap* was overexpressed (Figures 6M and 6N). ChIP was used to detect whether YAP binds to the promoter region of *CyclinD1*. The results showed that when *Yap* was overexpressed, the amount of YAP that bound to −0.2-kb region (R1′) of the *CyclinD1* promoter was increased (Figures 6O and S5B); the positive region R1′ was selected based on a previous study (Mizuno et al., 2012). The region of R2′ was randomly selected as a negative unrelated region. Further analysis showed that the immunostaining for pCREB, YAP, and CYCLIND1 was enhanced when *Grm7* was silenced (Figures S4D–S4I).

To support the roles of CREB, YAP, and CYCLIND1 in the regulation of neurogenesis, we performed immunostaining for CREB, phospho-CREB, YAP, and CYCLIND1 in the developing neocortex at E12.5, E15.5, and E18.5. Our results showed that CREB was expressed in the entire cortex

Figure 6. GRM7 Regulates CREB and YAP Signaling

(A and B) GRM7 regulates the phosphorylation of CREB and the expression of YAP. N2a cells were transfected with the *Grm7*-shRNA plasmid (A) or the *Grm7* overexpression plasmid (B) or the respective control. The phosphorylation of CREB was determined by immunoblotting with a phospho-CREB (Ser133) (pCREB)-specific antibody. The expression of YAP was determined by immunoblotting with a YAP-specific antibody (n = 3 independent experiments; β-ACTIN was used as a loading control; *p < 0.05, **p < 0.01; error bars represent mean ± SEM).

(C) CaM regulates the phosphorylation CREB and the expression of YAP. N2a cells were transfected with the control or *CaM* overexpression plasmid. CREB phosphorylation and YAP expression were determined via western blot (n = 3 independent experiments; β-ACTIN was used as a loading control; *p < 0.05, **p < 0.01; error bars represent mean ± SEM).

(D) GRM7 and CaM regulate CREB phosphorylation. N2a cells were transfected with the control or *CaM* overexpression plasmid or co-transfected with the *Grm7* and *CaM* overexpression plasmids. CREB phosphorylation was determined via western blot (n = 3 independent experiments; β-ACTIN was used as a loading control; *p < 0.05, **p < 0.01; error bars represent mean ± SEM).

(E and F) CREB regulates the expression of YAP. N2a cells were transfected with the control or CREB overexpression plasmid. The CREB, pCREB, and YAP levels were determined via western blot (n = 3 independent experiments; β-ACTIN was used as a loading control; *p < 0.05, **p < 0.01; error bars represent mean ± SEM).

(G and H) YAP acts downstream of CREB. The control, *Grm7* shRNA, *Creb* overexpression, *Creb* overexpression and *Yap* shRNA, *YAP-S127A*, or *YAP-S127A* and *Creb* shRNA plasmids were electroporated into E13.5 embryonic mouse brains, and the mice were sacrificed at E16.5. The percentage of GFP-positive cells in each region is shown (n = 3 independent experiments; *p < 0.05, **p < 0.01; error bars represent mean ± SEM). The scale bar represents 50 μm.

(I and J) *Grm7* knockdown causes YAP accumulation in the nucleus. N2a cells were transfected with the control shRNA or *Grm7*shRNA-2. The transfected cells were fixed two days later, and the cells were immunostained with an anti-YAP antibody (n = 4 independent experiments; *p < 0.05, **p < 0.01; error bars represent mean ± SEM). The scale bar represents 5 μm.

(K) CREB regulates the expression of YAP by binding to the *Yap* promoter. N2a cells were transfected with the control or *Creb* overexpression plasmid. The binding of CREB to the *Yap* promoter was determined via ChIP and real-time PCR (n = 3 independent experiments; *p < 0.05, **p < 0.01; error bars represent mean ± SEM).

(L) CaM was immunoprecipitated by GRM7, but not by GRM7-CD. Protein lysates were divided into two parts, one for the control IP and the other for the GRM7 IP. The immunoprecipitated proteins were probed with anti-Flag antibodies to detect Flag-CaM.

(M) *Grm7* knockdown increases the expression of *CyclinD1*. N2a cells were transfected with the control or *Grm7* shRNA plasmid. The relative *CyclinD1* mRNA level was detected via real-time PCR (n = 3 independent experiments; *p < 0.05, **p < 0.01; error bars represent mean ± SEM).

(N) *Yap* overexpression increases the expression of *CyclinD1*. N2a cells were transfected with the control or *Yap* overexpression plasmid. The relative *CyclinD1* mRNA level was detected via real-time PCR (n = 3 independent experiments; *p < 0.05, **p < 0.01; error bars represent mean ± SEM).

(O) YAP regulates the expression of *CyclinD1* by binding to the *CyclinD1* promoter. N2a cells were transfected with the control or *Yap* overexpression plasmid. The binding of YAP to the *CyclinD1* promoter was determined via ChIP and real-time PCR (n = 3 independent experiments; *p < 0.05, **p < 0.01; error bars represent mean ± SEM).

See also Figures S4 and S5.

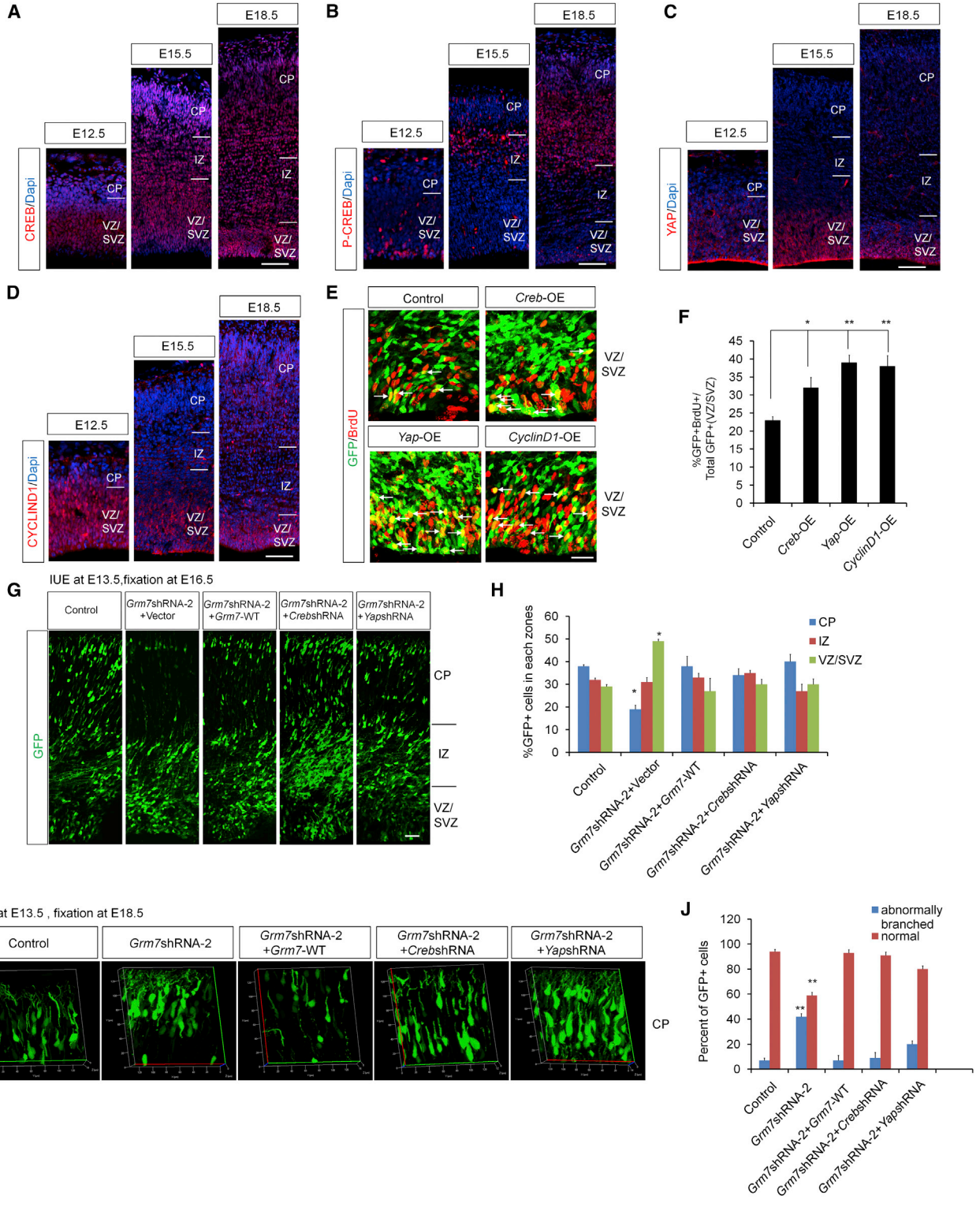

Figure 7. The Neurogenesis Defects Caused by *Grm7* Knockdown Could Be Ameliorated

(A–D) The expression patterns of CREB, pCREB, YAP, and CYCLIND1 support their roles in the regulation of neurogenesis. Cortical sections of E12.5, E15.5, and E18.5 mice were collected and immunostained for CREB, pCREB, YAP, and CYCLIND1. The scale bar represents 60 μm.

(legend continued on next page)

at different developmental stages. Phospho-CREB was expressed in the VZ/SVZ at E12.5 and accumulated in the IZ and the CP at E15.5 and E18.5, and a subset pCREB-positive cells remained in the VZ/SVZ at E15.5 and E18.5. This expression pattern is consistent with a previous report that pCREB is involved in the process of proliferation and consistently participates in the process of differentiation (Mantamadiotis et al., 2012). YAP and CYCLIND1 were expressed in the VZ/SVZ of the brain, consistent with their role in promoting proliferation (Figures 7A–7D).

Our results of phenotypic analysis following IUE showed that *Grm7* overexpression, *Creb* knockdown, or *Yap* knockdown ameliorated the defects in neurogenesis caused by *Grm7* knockdown (Figures 7G and 7H). These results indicate that CREB and YAP may act as downstream regulatory effectors of GRM7 signaling during early cortical development. To study whether *Creb* or *Yap* knockdown ameliorates these morphological changes, we performed IUE at E13.5 and phenotypic analysis at E18.5. The 3D reconstruction results also showed that *Creb* or *Yap* knockdown ameliorates these morphological changes (Figures 7I and 7J).

DISCUSSION

GRM7 may be associated with brain developmental disorders, including ADHD (Elia et al., 2012) and ASD (Yang and Pan, 2013). However, there is no direct evidence regarding whether or how GRM7 regulates brain development and neurogenesis. Neurogenesis in the developing brain is dynamically regulated by multiple factors and pathways. Here, we provide several lines of evidence demonstrating that GRM7 is essential for brain cortical neurogenesis. These data indicate a role of GRM7 in the developing mammalian cortex. Our results may provide an understanding of the genetic mechanism underlying brain pathophysiology and may reveal potential targets for therapeutic intervention.

Metabotropic glutamate receptors, which contain seven transmembrane domains, belong to the G protein-coupled receptor family, which is actively involved in brain development and function (Conn and Pin, 1997). GRM7 is a type III GRM family member, and increasing evidence indicates that the mutation of GRM7 is closely correlated with brain diseases (Elia et al., 2012; Yang and Pan, 2013). The activation of GRM7 by glutamate depends on its membrane localization. Previous studies have shown that both PICK1 binding and PKC phosphorylation are required for the stable surface expression of GRM7 (Dev et al., 2000; Suh et al., 2008). Our results show that GRM7 is required for embryonic cortical development. Using IUE, we determined that *Grm7* knockdown leads to neurogenesis defects, including increased proliferation and decreased differentiation of NPCs. *Grm7* knockdown results in decreased premature NPC terminal mitosis. We provide evidence that GRM7 is essential for neuronal morphofunctional changes and maturation.

Previous studies have shown that CREB (Mantamadiotis et al., 2012) and YAP (Vassilev et al., 2001) are critical modulators of the process of brain development. It is known that some G protein-coupled receptors activate the cAMP/CREB pathway (Neves et al., 2002). Because CREB and YAP regulate NSC proliferation, we hypothesized that GRM7 regulates neurogenesis via these signaling effectors. Our results demonstrated that GRM7 regulates neural progenitor proliferation and differentiation via the modulation of CREB phosphorylation at Ser133 and YAP expression. When GRM7 function was lost, the phosphorylation of CREB at Ser133 (active form) and the expression of YAP (active form) were increased. In our study, we also observed that when *Grm7* was silenced, the number of cells exiting the cell cycle ($GFP^+BrdU^+Ki67^-$) was decreased. We also found that when *Grm7* was silenced, the expression of *CyclinD1* was increased; a similar result was observed when *Yap* was overexpressed. The increase in the active YAP level caused by *Grm7* knockdown subsequently induced the expression of *CyclinD1*, which promoted NPCs proliferation; these events are consistent with the known function of YAP.

During early cortical development, the expression of GRM7 peaks at E15. The high expression of GRM7 at E15 suggests that it plays a critical role during this important

(E and F) BrdU incorporation is increased in *Creb*-, *Yap*-, or *CyclinD1*-overexpressing brains. The brains of mice were electroporated at E13.5, and BrdU was injected 2 hr prior to sacrificing the mice at E16.5. The arrows indicate GFP and BrdU double-positive cells. The bar graph shows the percentage of BrdU and GFP double-positive cells relative to the total GFP-positive cells in the VZ/SVZ (n = 3 independent experiments; *p < 0.05, **p < 0.01; error bars represent mean ± SEM). The scale bar represents 20 μm.

(G and H) *Grm7* overexpression, *Creb* knockdown, or *Yap* knockdown ameliorates the early neurogenesis defect caused by *Grm7* knockdown in utero. The indicated plasmids were electroporated into E13.5 embryonic mouse brains, and the mice were sacrificed at E18.5. The percentage of GFP-positive cells in each region is shown (n = 3 independent experiments; *p < 0.05, **p < 0.01; error bars represent mean ± SEM). The scale bar represents 50 μm.

(I and J) *Grm7* overexpression, *Creb* knockdown, or *Yap* knockdown ameliorates the morphological changes caused by *Grm7* knockdown. The indicated plasmids were electroporated into E13.5 embryonic mouse brains, and the mice were sacrificed at E18.5 (n = 3 independent experiments; *p < 0.05, **p < 0.01; error bars represent mean ± SEM).

period of neurogenesis, and this hypothesis is consistent with our findings. Our results also demonstrated that *Grm7* knockdown leads to cell morphological changes. Therefore, GRM7 may mediate neuronal morphofunctional changes and maturation, thus enabling mature neurons to integrate intracortical inputs.

In our study, using IUE, we demonstrated that *Grm7* knockdown leads to abnormal neuronal branching and distribution. Based on these morphological changes caused by *Grm7* knockdown, GRM7 may also participate in neuronal migration. The morphological change from a multipolar to a bipolar morphology is a crucial event that is coupled to the migration of the immature neuron from the VZ to the CP in an inside-out pattern. During brain development, the CREB protein has been associated with neuronal migration, and the phosphorylation of CREB at Ser133 is increased during the late phase of migration (Giachino et al., 2005). GRM7 may regulate neuronal migration by modulating CREB phosphorylation at Ser133. YAP regulates the proliferation and differentiation of NPCs; however, whether YAP is involved in neuronal migration has not been reported previously and requires further investigation.

In summary, we demonstrate that GRM7 functions as a modulator of neurogenesis. We identify CREB, YAP, and CYCLIND1 as the downstream targets of GRM7. The phosphorylation of CREB at Ser133 and the expression of YAP and *CyclinD1* are modulated by GRM7, thereby regulating neurogenesis. Future behavioral studies will facilitate a deeper understanding of the relationship between GRM7 and developmental brain disorders.

EXPERIMENTAL PROCEDURES

In Utero Electroporation

The detailed protocols have been previously described (Lv et al., 2014). Briefly, pregnant (E13.5) ICR (Institute of Cancer Research) mice were anesthetized with pentobarbital sodium and and the uterine horns were exposed. Then, 1 μl recombinant plasmid (final concentration 2 μg/μl) mixed with enhanced GFP plasmid (Venus-GFP) at a 3:1 mol ratio and fast green (2 μg/μl; Sigma) was microinjected into the mouse fetal brain ventricles with glass capillaries. Five electric pulses of 40 V for 50 ms were applied at intervals of 950 ms across the head using an electroporator and platinum electrodes (Manual BTX ECM830). Following electroporation, the mice were sacrificed at E14.5, E16.5, or E18.5 and used for phenotype analysis. The brains were dissected and fixed in 4% paraformaldehyde (PFA) overnight at 4°C and then dehydrated in 30% sucrose.

BrdU Labeling

For NPC proliferation analysis, BrdU (100 mg/kg) was administered to pregnant female mice 72 hr after electroporation via an intraperitoneal (i.p.) injection. The embryonic brains were collected for phenotype analysis after BrdU labeling for 2 hr as previously described (Singh et al., 2010).

For the cell-cycle exit experiment, BrdU (100 mg/kg) was administered to mice 2 days after electroporation via i.p. injection. After 24 hr, the mouse brains were separated and processed. Then, the brains were co-stained with anti-BrdU and anti-Ki67 antibodies for analysis as previously described (Mao et al., 2009; Singh et al., 2010).

For the premature NPC terminal mitosis experiment, BrdU (100 mg/kg) was administered to pregnant female mice 24 hr after electroporation via an i.p. injection. The embryonic brains were collected for phenotype analysis after BrdU labeling for 4 days as previously described (Gambello et al., 2003; Hasan et al., 2013).

Immunostaining

Coronal sections (15 μm) were harvested using a freezing microtome (Leica CM1950), and the brain sections were placed on the adhesion microscope slides for analysis according to a previous study (Mao et al., 2009). Immunohistochemistry (IHC) was done on 15-μm-thick coronal brain sections; the brain sections were washed with 1% PBST (1% Triton X-100 in 1 M PBS [pH 7.4]), fixed 30 min by 4% PFA, and washed by PBST for 15 min three times. The slices were incubated with blocking buffer (5% BSA in 1% PBST) for 1 hr at room temperature. When IHC was required for BrdU, the brain sections were washed using PBST for 15 min three times. Sequentially, the sections were subjected to HCl treatment, incubated in ice-cold 1 N HCl for 10 min, in 2 N HCl for 10 min at room temperature, and in 2 N HCl for 20 min at 37°C. After finishing the above steps, PBST was used to wash the sections three times. Blocking was processed as previously described. The brain slices were incubated in primary antibodies at 4°C overnight. The brain sections were then washed in PBST for 15 min three times followed by secondary antibodies conjugated with Alexa Fluor dyes (1:1,000 dilution; Jackson ImmunoResearch) in PBST buffer for 1 hr at room temperature. The brain sections were washed three times for 15 min in PBST, incubated with 2 μg/ml DAPI for 2 min, and washed three times for 5 min with PBST.

Immunostaining for cultured cells was performed according to the following procedure: the cells were washed with PBST (0.1% Triton X-100 in 1 M PBS), fixed in 4% PFA, blocked by 5% BSA (Sangon, in 0.1% PBST), incubated with primary antibodies overnight at 4°C, and visualized using fluorescence-labeling secondary antibodies.

Western Blotting and Co-immunoprecipitation

Cell pellets were lysed with RIPA (Solarbio) in combination with 10 mM PMSF and cocktail (Sigma) for 5 min on ice and then centrifuged for 5 min at 4°C to eliminate cell debris. Next, the protein samples (in 4× loading buffer) were loaded onto SDS-PAGE gels.

Subsequently, the protein bands were transferred to nitrocellulose or polyvinylidene fluoride membranes and blocked in 5% nonfat milk in PBS-T (PBS with 0.1% Tween-20) for 1 hr at room temperature. The membranes were then incubated at 4°C overnight with primary antibody and IRDye 800CW or 680CW (LI-COR Biosciences) donkey anti-mouse or anti-rabbit secondary antibodies were used to visualize the bands.

For co-immunoprecipitation, fresh extracted protein samples were incubated with 30 μl Dynabeads Protein A (Life Technology)

overnight at 4°C, which had been previously incubated with primary antibody (1 μl in PBS including 0.02% Tween-20). The Dynabeads-antibody-sample complex was washed three times to remove the supernatant using a magnet. 30 μl 1× loading buffer was added to the complex and then placed in 70°C water for 10 min for complex depolymerization. Next, the 20-μl supernatant was collected for western blotting.

RT-PCR

The total RNA was extracted by using the TRIzol (Invitrogen) according to the manufacturer's instructions. FastQuant RT Kit (with DNase, TIANGEN) was used to get first-strand cDNA. The primers used for real-time PCR were as follows: *CyclinD1*, 5′-GCCTACAGCCCTGTTACCTG-3′ (forward) and 5′-ATTTCATCCC TACCGCTGTG-3′ (reverse); *β-Actin*, 5′-GGTGGGAATGGGTCA GAAGG-3′ (forward) and 5′-AGGAAGAGGATGCGCCAGTG-3′ (reverse).

Confocal Imaging and Statistical Analysis

All images were captured with a Zeiss 780 laser scanning confocal microscope and analyzed with Photoshop CS4 (Adobe). Statistical analyses were performed using a one-way ANOVA or t test (*$p < 0.05$, **$p < 0.01$). All bar graphs are shown as the means ± SEM, and error bars represent mean ± SEM.

SUPPLEMENTAL INFORMATION

Supplemental Information includes Supplemental Experimental Procedures and five figures and can be found with this article online at http://dx.doi.org/10.1016/j.stemcr.2015.03.004.

AUTHOR CONTRIBUTIONS

W.X., Y.L., and J.J. designed the research; W.X. and Y.L. performed the research and analyzed the data; and W.X., Y.L., and J.J. wrote the manuscript.

ACKNOWLEDGMENTS

We thank Junhua Lv and Feng Liu for technical help. This work was supported by grants from the National Key Basic Research Program of China (2015CB964501 and 2014CB964903), Strategic Priority Research Program (XDA01020301), and the National Science Foundation of China (31371477).

Received: October 9, 2014
Revised: March 19, 2015
Accepted: March 20, 2015
Published: April 23, 2015

REFERENCES

Bradley, S.R., Levey, A.I., Hersch, S.M., and Conn, P.J. (1996). Immunocytochemical localization of group III metabotropic glutamate receptors in the hippocampus with subtype-specific antibodies. J. Neurosci. *16*, 2044–2056.

Cai, J., Zhang, N., Zheng, Y., de Wilde, R.F., Maitra, A., and Pan, D. (2010). The Hippo signaling pathway restricts the oncogenic potential of an intestinal regeneration program. Genes Dev. *24*, 2383–2388.

Cao, X., Pfaff, S.L., and Gage, F.H. (2008). YAP regulates neural progenitor cell number via the TEA domain transcription factor. Genes Dev. *22*, 3320–3334.

Conn, P.J., and Pin, J.P. (1997). Pharmacology and functions of metabotropic glutamate receptors. Annu. Rev. Pharmacol. Toxicol. *37*, 205–237.

Das, D., Lanner, F., Main, H., Andersson, E.R., Bergmann, O., Sahlgren, C., Heldring, N., Hermanson, O., Hansson, E.M., and Lendahl, U. (2010). Notch induces cyclin-D1-dependent proliferation during a specific temporal window of neural differentiation in ES cells. Dev. Biol. *348*, 153–166.

Dev, K.K. (2004). Making protein interactions druggable: targeting PDZ domains. Nat. Rev. Drug Discov. *3*, 1047–1056.

Dev, K.K., Nakajima, Y., Kitano, J., Braithwaite, S.P., Henley, J.M., and Nakanishi, S. (2000). PICK1 interacts with and regulates PKC phosphorylation of mGLUR7. J. Neurosci. *20*, 7252–7257.

Duque, A., and Rakic, P. (2011). Different effects of bromodeoxyuridine and [3H]thymidine incorporation into DNA on cell proliferation, position, and fate. J. Neurosci. *31*, 15205–15217.

Dworkin, S., Heath, J.K., deJong-Curtain, T.A., Hogan, B.M., Lieschke, G.J., Malaterre, J., Ramsay, R.G., and Mantamadiotis, T. (2007). CREB activity modulates neural cell proliferation, midbrain-hindbrain organization and patterning in zebrafish. Dev. Biol. *307*, 127–141.

Elia, J., Glessner, J.T., Wang, K., Takahashi, N., Shtir, C.J., Hadley, D., Sleiman, P.M., Zhang, H., Kim, C.E., Robison, R., et al. (2012). Genome-wide copy number variation study associates metabotropic glutamate receptor gene networks with attention deficit hyperactivity disorder. Nat. Genet. *44*, 78–84.

Fernandez-L, A., Northcott, P.A., Dalton, J., Fraga, C., Ellison, D., Angers, S., Taylor, M.D., and Kenney, A.M. (2009). YAP1 is amplified and up-regulated in hedgehog-associated medulloblastomas and mediates Sonic hedgehog-driven neural precursor proliferation. Genes Dev. *23*, 2729–2741.

Gal, J.S., Morozov, Y.M., Ayoub, A.E., Chatterjee, M., Rakic, P., and Haydar, T.F. (2006). Molecular and morphological heterogeneity of neural precursors in the mouse neocortical proliferative zones. J. Neurosci. *26*, 1045–1056.

Gambello, M.J., Darling, D.L., Yingling, J., Tanaka, T., Gleeson, J.G., and Wynshaw-Boris, A. (2003). Multiple dose-dependent effects of Lis1 on cerebral cortical development. J. Neurosci. *23*, 1719–1729.

Gee, S.T., Milgram, S.L., Kramer, K.L., Conlon, F.L., and Moody, S.A. (2011). Yes-associated protein 65 (YAP) expands neural progenitors and regulates Pax3 expression in the neural plate border zone. PLoS ONE *6*, e20309.

Giachino, C., De Marchis, S., Giampietro, C., Parlato, R., Perroteau, I., Schutz, G., Fasolo, A., and Peretto, P. (2005). cAMP response element-binding protein regulates differentiation and survival of newborn neurons in the olfactory bulb. J. Neurosci. *25*, 10105–10118.

Götz, M., and Huttner, W.B. (2005). The cell biology of neurogenesis. Nat. Rev. Mol. Cell Biol. *6*, 777–788.

Hasan, S.M., Sheen, A.D., Power, A.M., Langevin, L.M., Xiong, J., Furlong, M., Day, K., Schuurmans, C., Opferman, J.T., and Vanderluit, J.L. (2013). Mcl1 regulates the terminal mitosis of neural precursor cells in the mammalian brain through p27Kip1. Development *140*, 3118–3127.

Lian, I., Kim, J., Okazawa, H., Zhao, J., Zhao, B., Yu, J., Chinnaiyan, A., Israel, M.A., Goldstein, L.S., Abujarour, R., et al. (2010). The role of YAP transcription coactivator in regulating stem cell self-renewal and differentiation. Genes Dev. *24*, 1106–1118.

Lv, X., Jiang, H., Liu, Y., Lei, X., and Jiao, J. (2014). MicroRNA-15b promotes neurogenesis and inhibits neural progenitor proliferation by directly repressing TET3 during early neocortical development. EMBO Rep. *15*, 1305–1314.

Mantamadiotis, T., Papalexis, N., and Dworkin, S. (2012). CREB signalling in neural stem/progenitor cells: recent developments and the implications for brain tumour biology. Bioessays *34*, 293–300.

Mao, Y., Ge, X., Frank, C.L., Madison, J.M., Koehler, A.N., Doud, M.K., Tassa, C., Berry, E.M., Soda, T., Singh, K.K., et al. (2009). Disrupted in schizophrenia 1 regulates neuronal progenitor proliferation via modulation of GSK3beta/beta-catenin signaling. Cell *136*, 1017–1031.

McConnell, S.K. (1995). Constructing the cerebral cortex: neurogenesis and fate determination. Neuron *15*, 761–768.

Mizuno, T., Murakami, H., Fujii, M., Ishiguro, F., Tanaka, I., Kondo, Y., Akatsuka, S., Toyokuni, S., Yokoi, K., Osada, H., and Sekido, Y. (2012). YAP induces malignant mesothelioma cell proliferation by upregulating transcription of cell cycle-promoting genes. Oncogene *31*, 5117–5122.

Neves, S.R., Ram, P.T., and Iyengar, R. (2002). G protein pathways. Science *296*, 1636–1639.

Nowakowski, R.S., Lewin, S.B., and Miller, M.W. (1989). Bromodeoxyuridine immunohistochemical determination of the lengths of the cell cycle and the DNA-synthetic phase for an anatomically defined population. J. Neurocytol. *18*, 311–318.

Rakic, P. (1995). A small step for the cell, a giant leap for mankind: a hypothesis of neocortical expansion during evolution. Trends Neurosci. *18*, 383–388.

Schlett, K. (2006). Glutamate as a modulator of embryonic and adult neurogenesis. Curr. Top. Med. Chem. *6*, 949–960.

Singh, K.K., Ge, X., Mao, Y., Drane, L., Meletis, K., Samuels, B.A., and Tsai, L.H. (2010). Dixdc1 is a critical regulator of DISC1 and embryonic cortical development. Neuron *67*, 33–48.

Stachowiak, E.K., Fang, X., Myers, J., Dunham, S., and Stachowiak, M.K. (2003). cAMP-induced differentiation of human neuronal progenitor cells is mediated by nuclear fibroblast growth factor receptor-1 (FGFR1). J. Neurochem. *84*, 1296–1312.

Suh, Y.H., Pelkey, K.A., Lavezzari, G., Roche, P.A., Huganir, R.L., McBain, C.J., and Roche, K.W. (2008). Corequirement of PICK1 binding and PKC phosphorylation for stable surface expression of the metabotropic glutamate receptor mGluR7. Neuron *58*, 736–748.

Vassilev, A., Kaneko, K.J., Shu, H., Zhao, Y., and DePamphilis, M.L. (2001). TEAD/TEF transcription factors utilize the activation domain of YAP65, a Src/Yes-associated protein localized in the cytoplasm. Genes Dev. *15*, 1229–1241.

Wang, J., Ma, L., Weng, W., Qiao, Y., Zhang, Y., He, J., Wang, H., Xiao, W., Li, L., Chu, Q., et al. (2013). Mutual interaction between YAP and CREB promotes tumorigenesis in liver cancer. Hepatology *58*, 1011–1020.

Xu, D., Zhang, F., Wang, Y., Sun, Y., and Xu, Z. (2014). Microcephaly-associated protein WDR62 regulates neurogenesis through JNK1 in the developing neocortex. Cell Rep. *6*, 104–116.

Yang, Y., and Pan, C. (2013). Role of metabotropic glutamate receptor 7 in autism spectrum disorders: a pilot study. Life Sci. *92*, 149–153.

Zhang, H., Deo, M., Thompson, R.C., Uhler, M.D., and Turner, D.L. (2012). Negative regulation of Yap during neuronal differentiation. Dev. Biol. *361*, 103–115.

Zhang, C., Mejia, L.A., Huang, J., Valnegri, P., Bennett, E.J., Anckar, J., Jahani-Asl, A., Gallardo, G., Ikeuchi, Y., Yamada, T., et al. (2013). The X-linked intellectual disability protein PHF6 associates with the PAF1 complex and regulates neuronal migration in the mammalian brain. Neuron *78*, 986–993.